Electronic Supplementary Information for *New Journal of Chemistry*

Synthesis, crystal structures and magnetic properties of a series of pentanuclear heterometallic [$Cu^{II}_3Ln^{III}_2$] (Ln = Ho, Dy, Gd) complexes containing mixed organic ligands†

Yong Chen,[a] Qiao-Qiao Long,[a] Zhao-Bo Hu,[b] Hui-Sheng Wang,[*a] Zhi-Yong Huang,[a] Wei Chen,[a] You Song,[*b] Zai-Chao Zhang[*c] and Feng-Jun Yang[a]

[a]School of Chemistry and Environmental Engineering, Key Laboratory of Green Chemical Process of Ministry of Education, Wuhan Institute of Technology, Wuhan 430074, P. R. China. Fax: +86-27-87194560
[b]State Key Laboratory of Coordination Chemistry, School of Chemistry and Chemical Engineering, Collaborative Innovation Center of Advanced Microstructures, Nanjing University, Nanjing 210046, P. R. China.
Jiangsu Key Laboratory for the Chemistry of Low-dimensional Materials, School of Chemistry and Chemical Engineering, Huaiyin Normal University, P. R. China.
E-mail:wangch198201@163.com (H. S. Wang), yousong@nju.edu.cn (Y. Song), E-mail: 6199128@qq.com (Z. C. Zhang).

Table S1.Crystal data and structure refinements for **1–3**

compounds	**1**	**2**	**3**
Formula	$C_{58}H_{83}Cl_2Cu_3Ho_2N_{17}O_{15}$*	$C_{56}H_{78}Cl_2Cu_3Dy_2N_{16}O_{14}$	$C_{58}H_{81}Cl_2Cu_3Gd_2N_{17}O_{14}$
Color	green	green	green
Formula weight	1849.79*	1785.86	1816.41
Temperature	173(2)	173(2)	173(2)
Wavelength (nm)	0.71073	0.71073	0.71073
Crystal system	Monoclinic	Monoclinic	Monoclinic
Space group	$P2_1/n$	$P2_1/n$	$P2_1/n$
a (nm)	12.3525(4)	12.3998(6)	12.3998(6)
b (nm)	20.1759(8)	20.2013(8)	20.2013(8)
c (nm)	28.1711(11)	28.1694(12)	28.1694(12)
α (°)	90	90	90
β (°)	91.0180(10)	90.9270(10)	90.9270(10)
γ (°)	90	90	90
V(Å^3)	7019.8(5)	7055.3(5)	7055.3(5)
Z	4	4	4
D_c (g/cm^{-3})	1.750	1.681	1.71
Absorption coefficient	3.273	3.127	2.892
F(000)	3700	3564	3636
Crystal size (mm)	0.34× 0.17 × 0.07	0.33× 0.19 × 0.02	0.22× 0.13 × 0.08
θ range (°)	2.9640~25.3712	2.8824~25.3027	2.7453~25.3647
Limiting indices	−14≤ h ≤ 14	−14≤ h ≤ 14	−13≤ h ≤ 14
	−23≤ k ≤ 23	−20≤ k ≤ 24	−24≤ k ≤ 21
	−33≤ l≤ 33	−33≤ l≤ 33	−33≤ l≤ 33
Reflections collected	8922	8476	8214
Data / restraints / parameters	12322/18/882	12322/0/844	12323/21/872
Goodness-of-fit on F^2	1.028	1.027	1.076
Final R indices [I>2sigma(I)]	R_1 =0.0466	R_1 = 0.0531	R_1 = 0.0702
	wR_2 =0.0762	wR_2 = 0.0899	wR_2 = 0.0990
R indices (all data)	R_1 = 0.0826	R_1 = 0.0960	R_1 = 0.1204
	wR_2 = 0.0832	wR_2 = 0.0978	wR_2 = 0.1078
s (all data)	1.031	1.027	1.077

* The formula and formula weight for **1** include solvent H_2O with 73.40% occupancy in the crystal lattice. [a]$R_1 = \Sigma(||F_o| - |F_c||)/\Sigma|F_o|$. [b] $wR_2 = [\Sigma[w(F_o^2 - F_c^2)^2]/\Sigma[w(F_o^2)^2]]^{1/2}$, $w = 1/[\sigma^2(F_o^2)\ (ap)^2 + bp]$, where $p = [\max(F_o^2, 0) + 2F_c^2]/3$.

Table S2. Selected bond lengths (Å) and angles (°) for complex **1**

Bond lengths			
Cu(1)-O(1)	1.919(4)	Ho(1)-O(10)	2.282(4)
Cu(1)-O(5)	1.900(4)	Ho(1)-O(9)	2.321(4)
Cu(1)-N(1)	1.987(5)	Ho(1)-O(2)	2.380(4)
Cu(1)-N(4)	1.957(5)	Ho(1)-N(9)	2.388(5)
Cu(2)-Cl(1)	2.591(2)	Ho(1)-O(11)	2.410(4)
Cu(2)-O(9)	1.936(4)	Ho(1)-N(7)	2.551(5)
Cu(2)-O(2)	1.944(4)	Ho(1)-O(4)	2.603(4)
Cu(2)-N(3)	1.938(6)	Ho(2)-O(10)	2.248(4)
Cu(2)-N(2)	2.046(5)	Ho(2)-O(13)	2.278(4)
Cu(3)-Cl(2)	2.627(3)	Ho(2)-O(12)	2.307(4)
Cu(3)-O(12)	1.942(4)	Ho(2)-O(6)	2.336(4)
Cu(3)-N(6)	1.949(5)	Ho(2)-N(12)	2.386(5)
Cu(3)-O(6)	1.961(4)	Ho(2)-O(14)	2.471(4)
Cu(3)-N(5)	2.047(5)	Ho(2)-N(8)	2.527(4)
Ho(1)-O(13)	2.253(4)	Ho(2)-O(8)	2.561(4)
Bond angles			
O(1)-Cu(1)-O(5)	172.12(19)	O(2)-Ho(1)-O(9)	65.20(14)
O(1)-Cu(1)-N(1)	89.8(2)	O(2)-Ho(1)-O(4)	61.49(13)
O(5)-Cu(1)-N(1)	88.5(2)	N(9)-Ho(1)-O(4)	71.29(16)
O(1)-Cu(1)-N(4)	89.6(2)	O(11)-Ho(1)-O(4)	88.19(14)
O(5)-Cu(1)-N(4)	92.5(2)	O(13)-Ho(1)-O(10)	69.39(14)
O(9)-Cu(2)-N(3)	165.6(3)	O(13)-Ho(1)-O(9)	92.63(15)
O(9)-Cu(2)-O(2)	81.50(17)	N(7)-Ho(1)-O(9)	68.84(19)
O(9)-Cu(2)-N(2)	100.82(19)	N(7)-Ho(1)-N(9)	88.93(18)
N(3)-Cu(2)-N(2)	83.3(2)	O(13)-Ho(2)-O(10)	69.55(13)
O(12)-Cu(3)-N(6)	171.5(2)	O(6)-Ho(2)-O(8)	62.65(14)
O(12)-Cu(3)-O(6)	81.74(17)	O(6)-Ho(2)-O(14)	71.93(14)
N(6)-Cu(3)-O(6)	90.13(19)	O(13)-Ho(2)-N(8)	67.74(15)
O(12)-Cu(3)-N(5)	101.82(18)	O(14)-Ho(2)-N(8)	68.04(14)
N(6)-Cu(3)-N(5)	84.6(2)	O(13)-Ho(2)-N(12)	81.05(17)
O(6)-Cu(3)-N(5)	156.2(2)	N(12)-Ho(2)-N(8)	87.23(17)

Table S3. Selected bond lengths (Å) and angles (°) for complex **2**

Bond lengths			
Cu(1)-O(5)	1.905(5)	Dy(1)-O(9)	2.331(5)
Cu(1)-O(1)	1.913(5)	Dy(1)-O(2)	2.391(5)
Cu(1)-N(1)	1.973(6)	Dy(1)-N(9)	2.406(6)
Cu(1)-N(4)	1.975(6)	Dy(1)-O(11)	2.420(5)
Cu(2)-O(9)	1.941(5)	Dy(1)-N(7)	2.559(6)
Cu(2)-O(2)	1.948(5)	Dy(1)-O(4)	2.607(5)
Cu(2)-N(3)	1.952(7)	Dy(2)-O(10)	2.265(5)
Cu(2)-N(2)	2.053(6)	Dy(2)-O(13)	2.284(4)
Cu(3)-O(12)	1.949(5)	Dy(2)-O(12)	2.317(5)
Cu(3)-O(6)	1.958(5)	Dy(2)-O(6)	2.351(5)
Cu(3)-N(6)	1.962(6)	Dy(2)-N(12)	2.399(7)
Cu(3)-N(5)	2.044(6)	Dy(2)-N(8)	2.536(5)
Dy(1)-O(13)	2.256(5)	Dy(2)-O(8)	2.574(5)
Dy(1)-O(10)	2.280(5)	Dy(2)-O(14)	2.493(5)
Bond angles			
O(5)-Cu(1)-N(1)	88.70(2)	O(10)-Dy(1)-N(7)	66.79(19)
O(1)-Cu(1)-N(1)	89.50(2)	O(9)-Dy(1)-N(7)	68.53(18)
O(5)-Cu(1)-N(4)	92.30(2)	N(9)-Dy(1)-N(7)	88.80(2)
O(1)-Cu(1)-N(4)	89.80(2)	O(11)-Dy(1)-N(7)	68.84(19)
O(9)-Cu(2)-O(2)	81.90(2)	O(13)-Dy(1)-O(4)	76.63(17)
O(2)-Cu(2)-N(3)	91.50(2)	N(9)-Dy(1)-O(4)	71.62(19)
O(9)-Cu(2)-N(2)	100.60(2)	O(11)-Dy(1)-O(4)	88.12(18)
N(3)-Cu(2)-N(2)	83.30(3)	O(10)-Dy(2)-O(13)	91.74(12)
O(12)-Cu(3)-O(6)	82.43(19)	O(13)-Dy(2)-O(12)	133.93(12)
O(6)-Cu(3)-N(6)	89.70(2)	O(12)-Dy(2)-O(6)	33.48(12)
O(12)-Cu(3)-N(5)	101.00(2)	O(6)-Dy(2)-N(12)	33.93(12)
N(6)-Cu(3)-N(5)	85.10(2)	O(6)-Dy(2)-O(8)	62.34(16)
O(13)-Dy(1)-O(10)	69.82(16)	N(12)-Dy(2)-O(14)	74.50(2)
O(13)-D(1)-O(9)	92.46(17)	N(14)-Dy(2)-O(8)	96.14(16)
O(2)-Dy(1)-N(9)	125.70(2)	N(12)-Dy(2)-N(8)	86.90(2)

Table S4. Selected bond lengths (Å) and angles (°) for complex **3**

Bond lengths			
Cu(1)-O(5)	1.901(6)	Gd(1)-O(9)	2.357(6)
Cu(1)-O(1)	1.912(6)	Gd(1)-O(2)	2.412(6)
Cu(1)-N(4)	1.961(8)	Gd(1)-N(9)	2.431(8)
Cu(1)-N(1)	1.972(8)	Gd(1)-O(11)	2.458(6)
Cu(2)-N(3)	1.930(9)	Gd(1)-N(7)	2.570(7)
Cu(2)-O(9)	1.931(6)	Gd(1)-O(4)	2.620(6)
Cu(2)-O(2)	1.940(6)	Gd(2)-O(10)	2.279(6)
Cu(2)-N(2)	2.043(7)	Gd(2)-O(13)	2.296(6)
Cu(3)-N(5)	2.049(7)	Gd(2)-O(12)	2.335(6)
Cu(3)-O(12)	1.934(6)	Gd(2)-O(6)	2.356(6)
Cu(3)-N(6)	1.951(8)	Gd(2)-N(12)	2.444(8)
Cu(3)-O(6)	1.954(6)	Gd(2)-N(14)	2.523(6)
Gd(1)-O(13)	2.286(6)	Gd(2)-N(8)	2.548(7)
Gd(1)-O(10)	2.309(6)	Gd(2)-O(8)	2. 569(6)
Bond angles			
O(5)-Cu(1)-N(4)	92.10(3)	O(9)-Gd(1)-O(11)	85.40(2)
O(1)-Cu(1)-N(4)	90.00(3)	O(2)-Gd(1)-O(11)	75.50(2)
O(5)-Cu(1)-N(1)	88.80(3)	N(9)-Gd(1)-O(11)	78.30(2)
O(1)-Cu(1)-N(1)	89.60(3)	O(10)-Gd(1)-N(7)	67.00(2)
N(3)-Cu(2)-O(2)	91.60(3)	O(9)-Gd(1)-N(7)	68.50(2)
O(9)-Cu(2)-O(2)	82.70(3)	O(13)-Gd(1)-O(2)	86.00(2)
N(3)-Cu(2)-N(2)	82.50(3)	N(9)-Gd(1)-N(7)	88.90(3)
O(9)-Cu(2)-N(2)	100.30(3)	O(6)-Gd(2)-O(14)	72.10(2)
O(12)-Cu(3)-O(6)	82.00(2)	O(12)-Gd(2)-O(14)	82.50(2)
N(6)-Cu(3)-O(6)	89.90(3)	N(12)-Gd(2)-O(14)	74.30(3)
O(12)-Cu(3)-N(5)	101.40(3)	O(13)-Gd(2)-N(8)	67.80(2)
N(6)-Cu(3)-N(5)	84.90(3)	O(12)-Gd(2)-N(8)	68.80(2)
O(13)-Gd(1)-O(10)	69.00(2)	N(12)-Gd(2)-N(8)	87.60(3)
O(13)-Gd(1)-O(9)	91.90(2)	O(14)-Gd(2)-N(8)	67.10(2)
O(10)-Gd(1)-O(9)	97.70(2)	O(10)-Gd(2)-O(8)	75.60(2)

Table S5. The possible geometries of nonacoordination metal centers

Geometry	Point group	Polyhedron
OP-8	D_{8h}	Octagon
HPY-8	C_{7v}	Heptagonal pyramid
HBPY-8	D_{6h}	Hexagonal bipyramid
CU-8	O_h	Cube
SAPR-8	D_{4d}	Square antiprism
TDD-8	D_{2d}	Triangular dodecahedron
JGBF-8	D_{2d}	Johnson-Gyrobifastigium (J26)
JETBPY-8	D_{3h}	Johnson-Elongated triangular bipyramid (J14)
JBTP-8	C_{2v}	Johnson-Biaugmentedtrigonal prism (J50)
BTPR-8	C_{2v}	Biaugmentedtrigonal prism
JSD-8	D_{2d}	Snub disphenoid (J84)
TT-8	T_d	Triakis tetrahedron
ETBPY-8	D_{3h}	Elongated trigonalbipyramid (see 8)

Table S6. Deviation parameters calculated by SHAPE from each ideal polyhedron for complexes **1-3**

Compounds	**1**		**2**		**3**	
Geometry	Ho1	Ho2	Dy1	Dy2	Gd1	Gd2
OP-8	33.268	34.791	33.307	34.721	33.509	34.629
HPY-8	22.816	21.771	22.870	21.788	22.887	21.773
HBPY-8	10.019	10.083	9.931	9.935	9.841	9.877
CU-8	5.995	4.749	6.020	4.677	5.987	4.622
SAPR-8	4.035	4.844	4.022	4.876	4.141	4.982
TDD-8	3.137	**2.191**	3.168	**2.198**	3.222	**2.338**
JGBF-8	10.514	12.763	10.489	12.894	10.409	12.903
JETBPY-8	21.866	22.241	21.867	22.345	22.010	22.233
JBTP-8	3.479	4.174	3.453	4.210	3.554	4.341
BTPR-8	**2.963**	3.420	**2.933**	3.435	**2.996**	3.514
JSD-8	4.947	6.338	4.940	6.347	5.083	6.477
TT-8	6.811	5.626	6.809	5.556	6.790	5.513
ETBPY-8	20.486	20.991	20.462	21.099	20.473	20.824

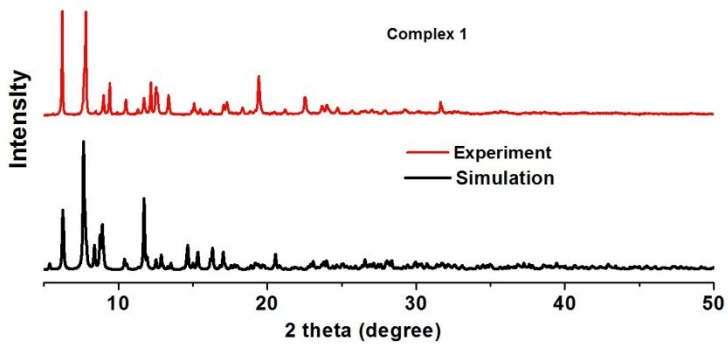

Figure S1. PXRD patterns and simulated patterns generated from single crystal diffraction data for compound **1**.

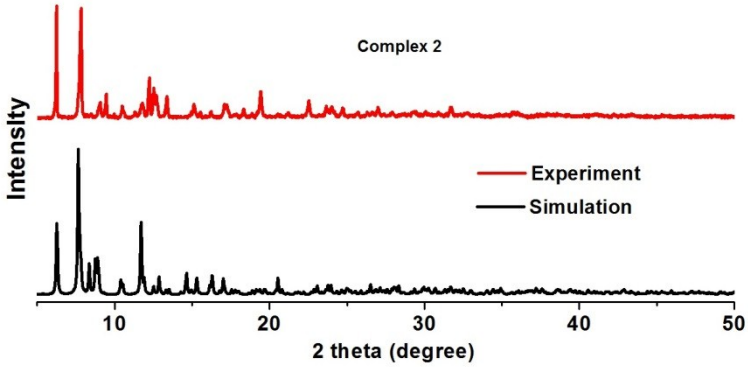

Figure S2. PXRD patterns and simulated patterns generated from single crystal diffraction data for compound **2**.

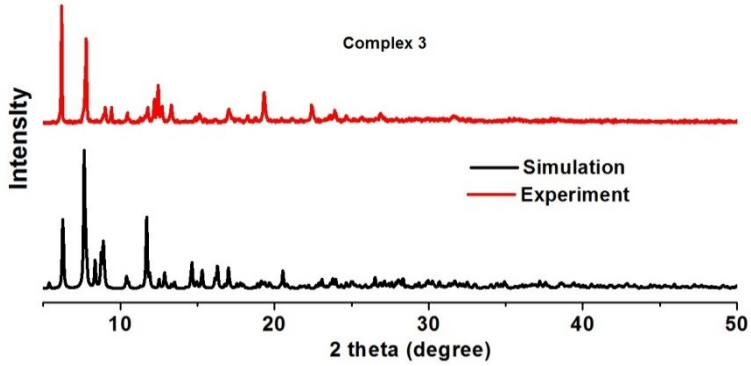

Figure S3. PXRD patterns and simulated patterns generated from single crystal diffraction data for compound **3**.

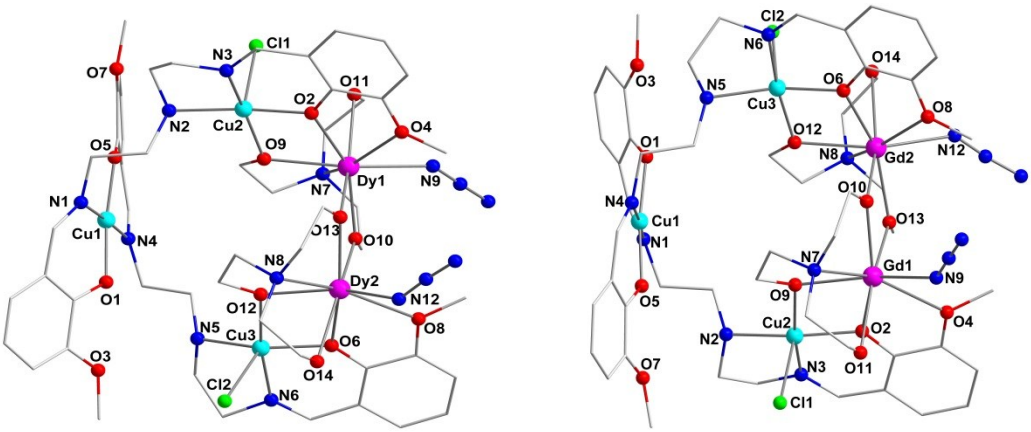

Figure S4. The molecular structure of $[Cu_3Dy_2(L)_2(teaH)_2(N_3)_2Cl_2]$ of **2** (left) and $[Cu_3Gd_2(L)_2(teaH)_2(N_3)_2Cl_2]$ (right) of **3** (Dy^{III} or Gd^{III} pink, Cu^{II} turquoise, N blue, O red, Cl bright green). For clarity, the H atoms and solvent molecules were omitted.

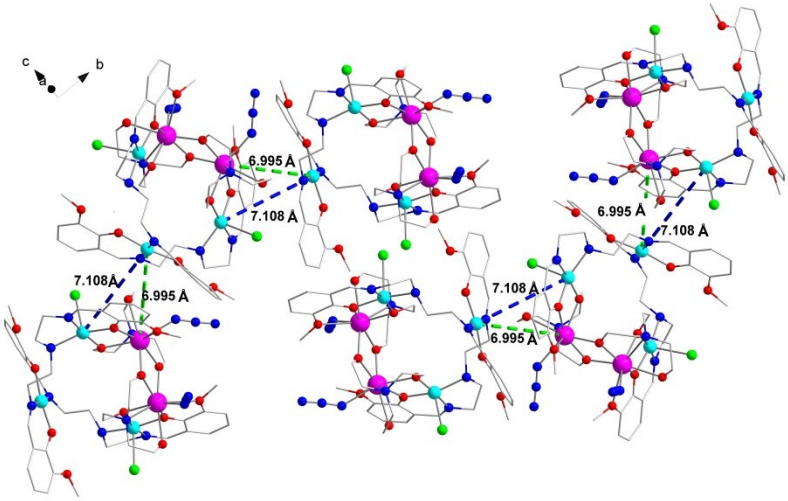

Figure S5. The plot shows the shortest distances of $Cu^{II}\cdots Cu^{II}$ and $Cu^{II}\cdots Ho^{III}$ between the nearest neighbor molecules of **1** (**(**Ho^{III} pink, Cu^{II} turquoise, N blue, O red, Cl bright green). For clarity, the H atoms and solvent molecules were omitted. Due to the structural similarities between **1** and **2**, **3**, the shortest distances were not shown for **2** and **3**.

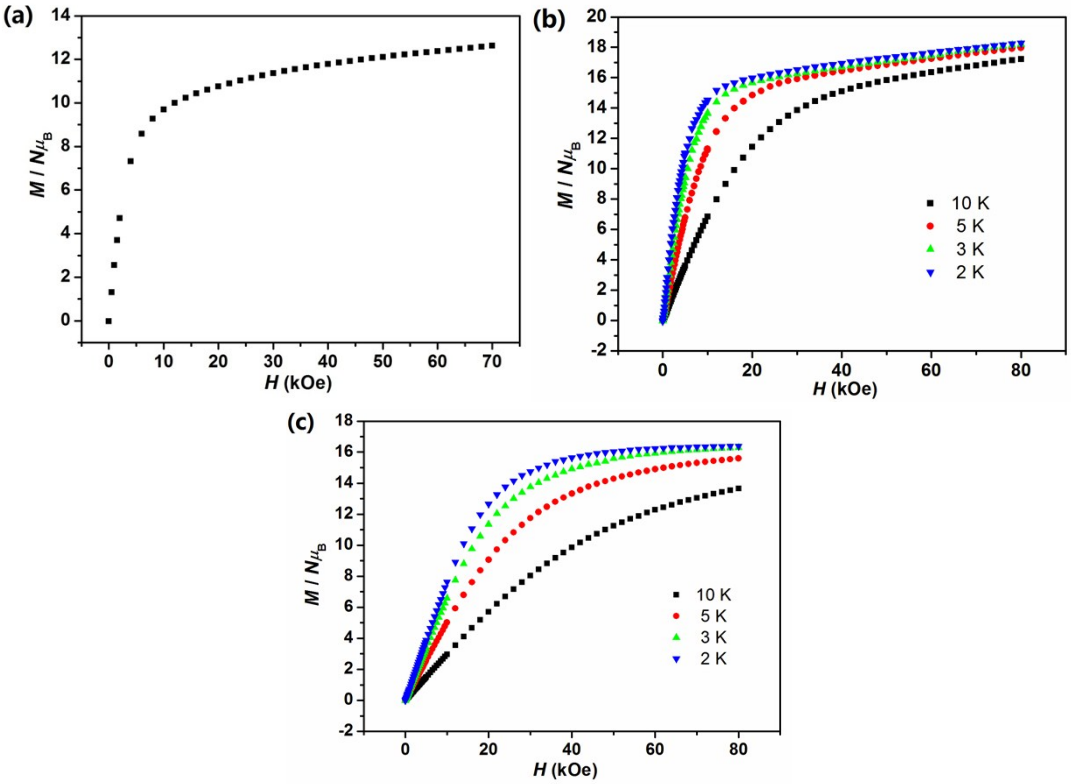

Figure S6. *M vs H* plots for compounds **1** (a) at 2 K, **2** (b) and **3** (c) at 2-10 K.

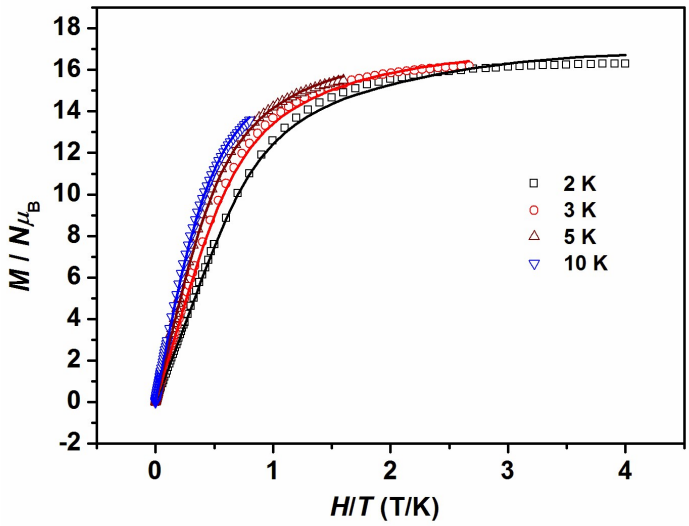

Figure S7 Plot of thee reduced magnetization (*M vs H*) for **3**. The solid lines represent the simulated results by PHI program.

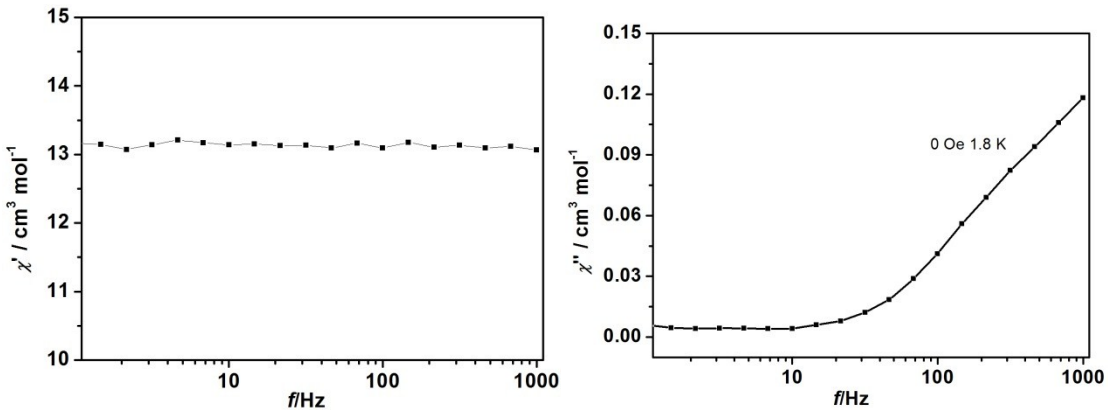

Figure S8. Frequency dependence of the in-phase (χ_M', left) and out-of-phase (χ'', right) ac magnetic susceptibilities for **1** collected under a 0 Oe dc field with the temperature 1.8.

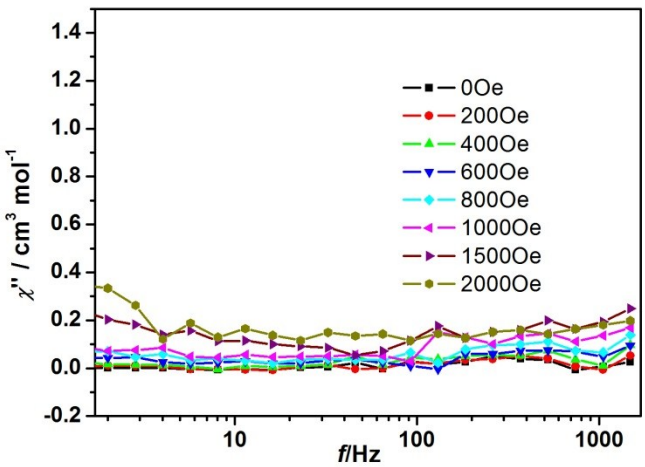

Figure S9. Plots of out-of-phase (χ'') versus *f* for **1** at 2.0 K with the dc fields ranging from 0 Oe to 2000 Oe and with the frequencies from 1 to 1488 Hz.

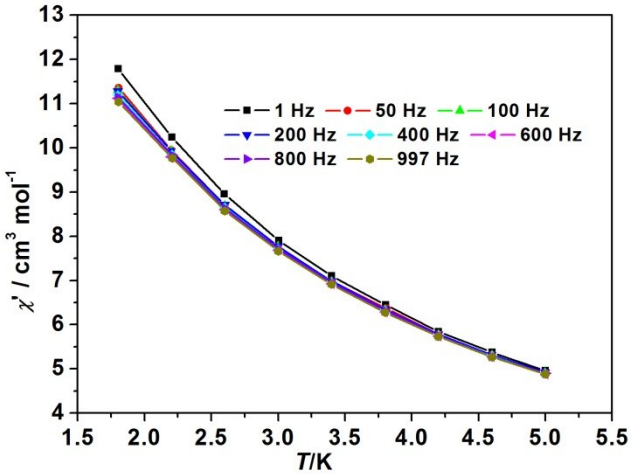

Figure S10. Plot of in-phase (χ') ac susceptibilities versus *T* for **1** at 1.8-5.0 K under 1000 Oe dc field with the frequency ranging from 1 to 999 Hz.

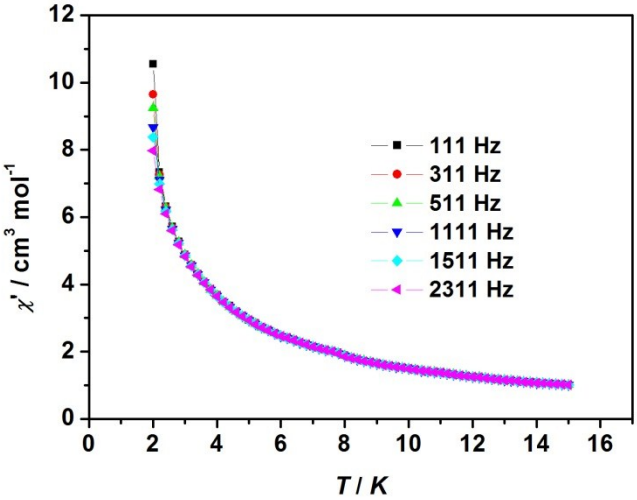

Figure S11. Plot of in-phase (χ') ac susceptibilities versus T for **2** at 2.0-15 K under 0 Oe dc field with the frequency ranging from 111 to 2311 Hz.

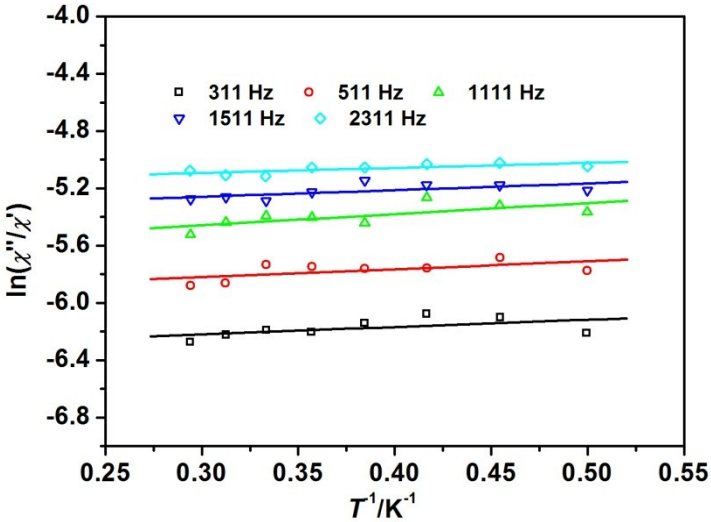

Figure S12 Plot of ln(χ''/χ') versus $1/T$ under 0 Oe dc field at different frequencies for complex **2**.

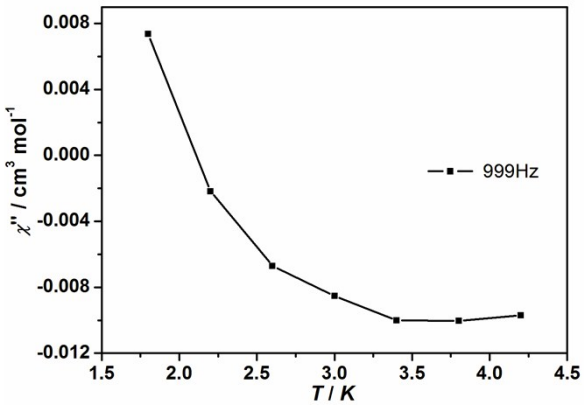

Figure S13.Temperature dependence of the out-of-phase (χ''_M) for **2** in a 5 Oe ac field oscillating at 999 Hz with a 1000 applied dc field.

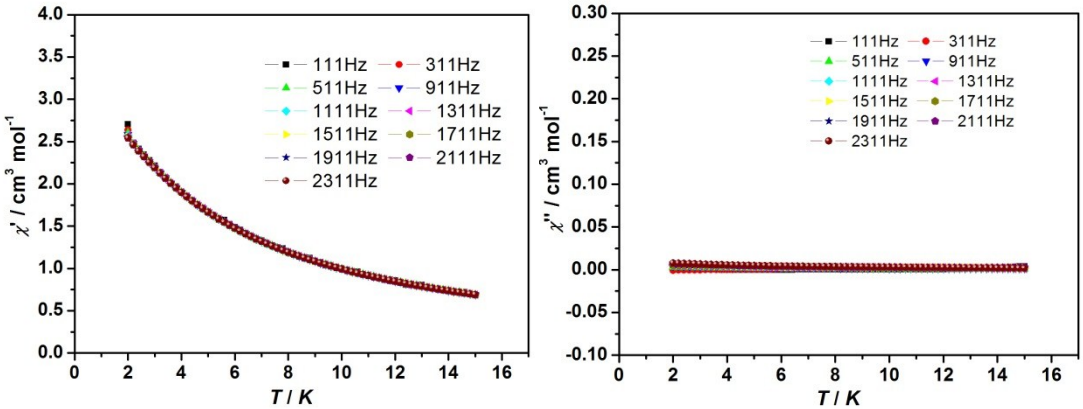

Figure S14. Plots of in-phase (χ′, left) and out-of-phase (χ″, right) ac susceptibilities versus *T* for **3** at 2.0-15 K under 0 Oe dc field with the frequency ranging from 111 to 2311 Hz.